GSA DATA REPOSITORY 2009206

Miner et al. Supplemental Material

Bathymetric Survey Methods

The bathymetric data for the area were gathered using a single-beam bathymetric survey rig mounted aboard a 21-foot shallow-draft survey vessel. This bathymetric survey rig consists of an *Odom Hydrographics Hydrotrac* system with a factory specified vertical resolution of 1.0 cm. Depth soundings are collected through a side-mounted *Odom Hydrographics* 200 kHz transducer with a beam width of 3°. Sound velocity was held constant at 1500 m s^{-1}. The fathometer is equipped with a *Starlink Invicta 210L* differential global positioning system (DGPS) for navigation. Heave, pitch, and roll of the transducer and DGPS antenna, arising from vessel motion, are recorded using a *VT TSS Dynamic Motion Sensor Series-25* that is mounted vertically in-line with the DGPS antenna and the transducer. The bathymetric, motion correction, and navigation data are simultaneously recorded digitally and integrated using *Coastal Oceanographics Hypack Max* hydrographic survey software run on an *Amrel Rocky Unlimited* field notebook computer.

Survey lines in the study area were programmed using *Hypack* and had ~500 – 800-m line spacing along shore-perpendicular transects. Shore-parallel tie-lines were also surveyed. During the actual survey, this spacing was not always followed in areas where shallow depths (-0.4 m) limited survey vessel accessibility or where shoal and island shorelines interfered with the completion of a planned line. When shallow depths along a shoal or island shoreline were encountered, the perimeter was mapped at the minimum depth accessible by the survey vessel (approximately -0.4 m). Bathymetric changes between the June and November surveys additionally required the alteration of survey transects in the field because shoaling between the two time frames locally limited vessel accessibility. Synthetic data points with a Z value of 0.5 m were digitized in for the islands and subaerial portions of the shoals on the basis of vertical aerial photography that was taken within a month of the bathymetric survey.

The bathymetric data were processed using *Hypack Single Beam Editor* module. Tidal elevation corrections were integrated using 6-minute interval data from NOAA tide gauge station # 8762075 located at Port Fourchon. The water level elevation from the tide gauge was measured relative to mean lower low water (MLLW), a tidal datum based on the National Tidal Datum Epoch 1983 –2001.

Gridding and Seafloor Change Analysis Methods

After processing, the bathymetric data were used to make a series of grids (node spacing = 100 m), which became the basis for the construction of digital elevation models (DEMs) for each survey time. The grids and DEMs were constructed using *Golden Software Sufer 8* contouring software. A kriging geostatistical algorithm was used to create the grids. Kriging is a distance weighting, moving average method that takes into account naturally occurring regional variables that are continuous from place to place (such as a linear bar or inlet channel), and assigns optimal weights on the basis of the geographic arrangement of data point Z values taken from a variogram (Davis, 1986; Krajewski and Gibbs, 2003). Kriging was determined to be the most appropriate contouring method because it takes into account spatial characteristics of the local geomorphology and provides the best linear estimate that can be obtained from an irregular arrangement of data samples. The grids created by the kriging method became the basis for contouring bathymetry and subsequent grid comparisons.

Grid math calculations were carried out between the two survey datasets (pre and post storms) to determine the difference between the November and June Z values at each grid node (e.g. November Z – June Z = net vertical change). This resulted in the creation of a new grid that showed areas of accretion and erosion through positive and negative values, respectively. A new DEM was contoured from these differential Z values in order to show changes (erosion, deposition, or dynamic equilibrium) that occurred during the 5-month time frame separating the two surveys. Volume calculations of the bathymetric change grid were computed in *Surfer 8* in order to determine positive volume (accretion) and negative volume (erosion).

Quantification of Uncertainty with Bathymetric Data and Seafloor Change Analysis

An error analysis was performed on the digital elevation models in order to document the accuracy of the bathymetry for Little Pass Timbalier and consequently the accuracy of the volume change calculations. Sources of uncertainty in the analyses include sounding errors, tidal corrections, and grid interpolation errors across the study area. Much of the uncertainty associated with human error during surveys is difficult to isolate and quantify, however, quality control measures such as comparison of soundings at line crossings and careful documentation of potential errors (e.g. bar-check velocity calibration of echosounder and transducer) during surveys helped to identify and limit the propagation of such errors. Tidal correction inaccuracies arise from indeterminate tidal elevation differences between the tide gauge at Port Fourchon and the study area. An approximation of water level differences between Little Pass Timbalier and Port Fourchon was calculated using the NOAA predicted water levels at each location during each survey. It was determined that the average time lapse for maximum and minimum water levels from Port Fourchon to Little Pass Timbalier was 25 minutes. Assuming a mean annual tide range of 0.30 m, the average difference in water level between the two locations is estimated to be 0.005 m. This value is considered to be an order of magnitude less than the values determined by the error analysis described below, and is therefore assumed to have little or no measurable effect on the outcome of the bathymetric change and volume calculations.

Survey line crossings are important to help identify potential equipment and human errors during the survey, as well as post-processing tidal corrections used to arrive at the measured Z value. In order to determine the accuracy of the tide-corrected measured depths, 10 survey line crossings (co-located soundings) from each survey were examined for differences in Z value. The crossings for the June data had an average difference in elevation of 0.05 m (+/- 0.025 m uncertainty) and 0.08 m (+/- 0.04 m uncertainty) for the November data. In order to determine the magnitude of the deviation the root mean square value for the two data sets was calculated and determined to be +/- 0.05 m. The line crossing uncertainty is not calculated as error and was only used to identify any large disparity at the crossings. The minor disparity observed at line crossings might be attributable to actual bathymetric changes because the surveys were carried out over multiple days.

A major source of uncertainty results from part of the gridding procedure involving synthetic data when z-values are interpolated for areas where no empirical bathymetric measurement was taken. In order to determine uncertainty with interpolated Z values, a grid calibration line was surveyed along an approximate 45° angle to the planned north-south trending survey lines (Supplementary Figs. DR1 and DR2). The grid calibration lines were chosen as transects that cross irregular bathymetry such as the ebb channel, channel margin bars, and ebb tidal delta. Before creating the entire study area grid, the data along the grid calibration line was removed from each data set. Grids were then created with the data points along these lines omitted. Bathymetric profiles through each of these modified grids, along the calibration line, were produced. The actual measured depth along the calibration line was then plotted against the profile from the modified grids to determine differences in cross sectional area between the grid surface profile and the measured data profile. The absolute value of the difference in the cross sectional area between the two lines was divided by the line distance to derive the average elevation difference between the two lines. The resulting value is the estimated range in uncertainty for the grid interpolations in areas where no data were acquired. For the June 2005 data, the cross-sectional area of the grid profile was 3901.80 m^2 and 4111.07 m^2 for the data profile, a difference of 209.27 m^2. By dividing the difference in cross sectional area by the line distance of 4000 m it was determined that there was an average elevation difference range of 0.052 m, or ± 0.026 m. For the November 2005 survey data the cross-sectional area of the grid profile was 5311.29 m^2 and 4970.91 m^2 for the data profile, a difference of 340.38 m^2. The difference in cross sectional areas divided by the length of the profile line of 4500 m results in an average elevation difference range of 0.076 m or ± 0.038 m.

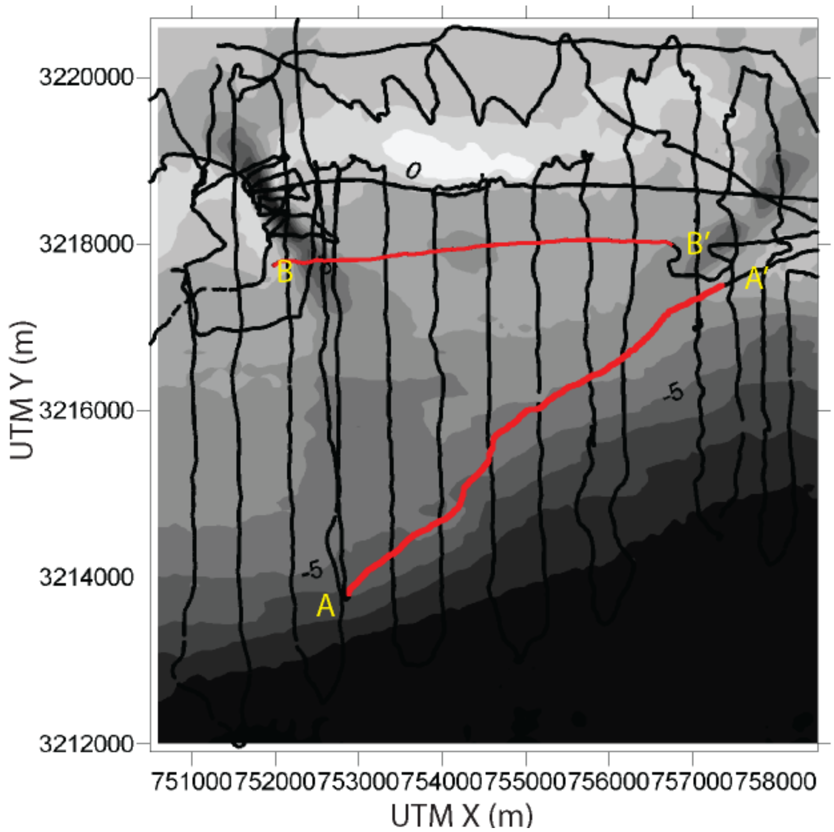

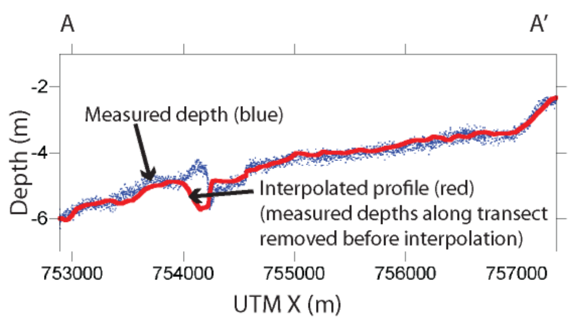

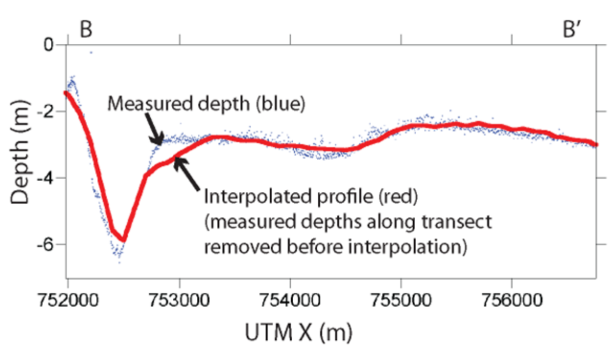

Supplementary Figure DR1. Bathymetric data coverage for June 2005 and grid interpolation transects used to quantify grid uncertainty at locations where no empirical data exist. Survey data (red) were removed from the dataset and new grids where created. Profiles along the grid where the survey lines were removed were compared to the measured data along the same line in order to access interpolation accuracy. Line A-A' was chosen because it trends across the ebb delta terminal lobe. The mean difference in elevation range along this profile is +/- 0.026 m. This value is applied as the vertical uncertainty for the June 2005 grid.

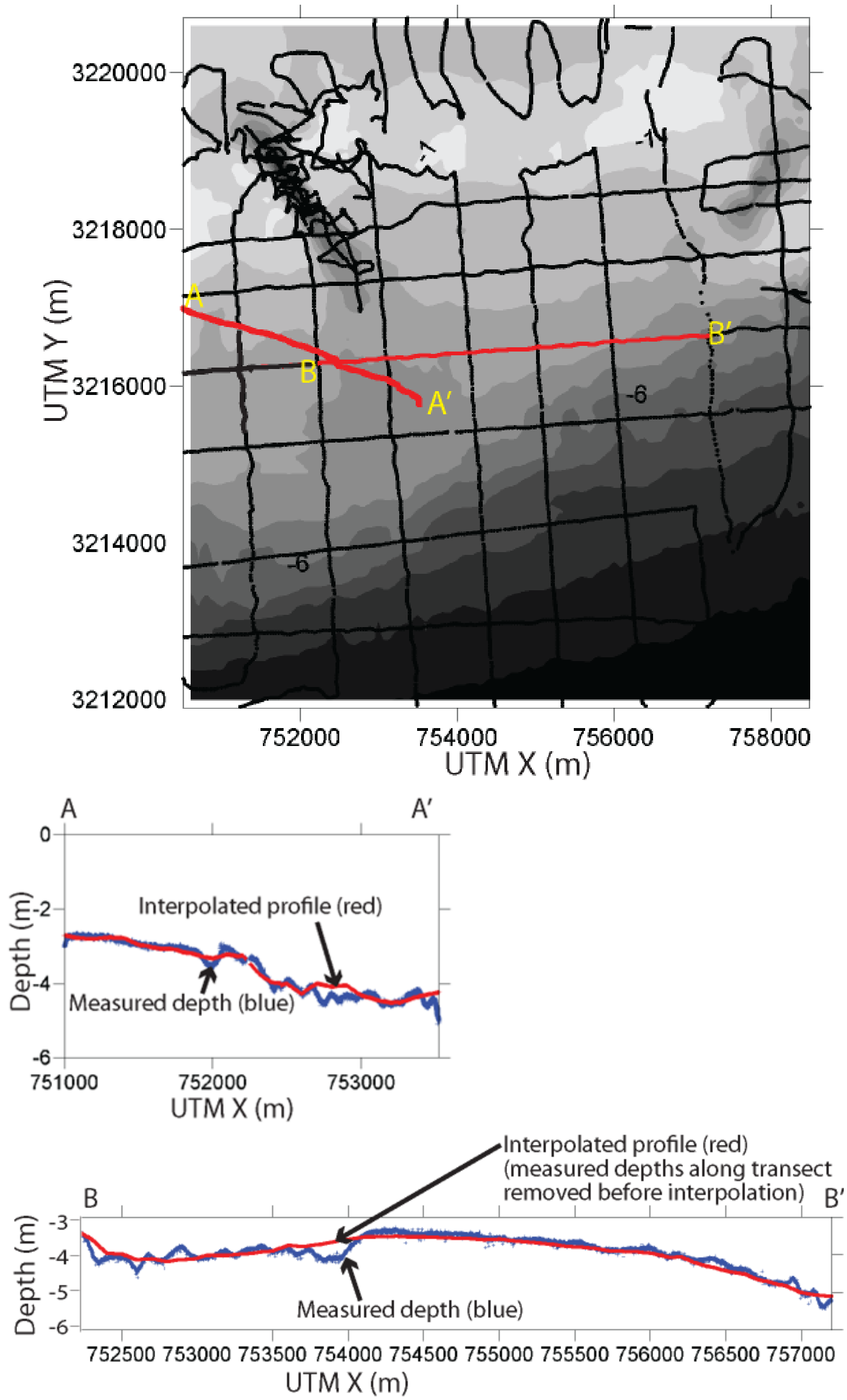

Supplementary Figure DR2. Bathymetric data coverage for November 2005 and grid interpolation transects used to quantify grid uncertainty at locations where no empirical data exist. Line A-A' was chosen because it trends across a varied topography that includes channel margin linear bars and the dredge pit discussed in the manuscript. The mean difference in elevation range along this profile is +/- 0.038 m. This value is applied as the vertical uncertainty for the November 2005 grid.

In order to determine the accuracy of the grid surface Z values relative to the measured soundings, the residuals (deviations of the grid surface Z value from the measured Z values) were computed using *Surfer 8*. For every measured Z value (>1.5 x 10^6 data points), a Z value for the grid surface is given. The mean difference between the data and the grid was 0.0072 m with a standard deviation of 0.23 for the June 2005 data and a mean difference of 0.0010 m with a standard deviation of 0.21 for the November 2005 data. Because these values are an order of magnitude smaller than the errors estimated by the grid calibration analysis, they are not included in the error uncertainty.

In order to determine the uncertainty in seafloor change and make sediment budget calculations, the root mean square (RMS) of the uncertainty values determined for each grid surface based on the grid calibration survey was calculated by

$$RMS = \sqrt{\sigma^2_{nov} + \sigma^2_{june}}, \qquad (1)$$

where σ_{nov} is the Z value uncertainty estimate for the November grid and σ_{june} is the Z value uncertainty estimate for the June grid as determined by the grid uncertainty analysis. The RMS value for the two grid sets is ± 0.05 m. This value was used as the uncertainty for the bathymetric change analysis and sediment volume change calculations. The uncertainty for the volume change calculations was determined by using the ± 0.05 m uncertainty Z value and multiplying it by the area in which the bathymetric change analysis study was conducted (47.9 km^2). Using this procedure, it was calculated that the maximum amount of error (for the entire study area) in the volumetric change analysis was ± 2.4 x 10^6 m^3.

Simulated Waves and Sand Transport Methods

Model setup, domain, and bathymetry

Wave simulations were performed using a steady-state, wave numerical model (STWAVE version 4; Smith et al., 2001). The model computational domain included a 23-meter resolution constant spacing Cartesian grid. Model bathymetry was interpolated from pre-storm conditions using the final grid prepared in *Surfer* for the June 2005 bathymetry.

Initial and Boundary conditions

Maximum sustained winds estimated/measured during the storms were used in the simulations (Smith, 2007; Oceanweather, 2006). The offshore boundary conditions for STWAVE were generated using the peak conditions simulated by Smith (2007) for hurricane Katrina and Oceanweather (2006) for hurricane Rita. The spectral density distribution at the boundary was accomplished with the Bretschneider (1959) approach, with the function peak set to the maximum conditions predicted by Smith (2007). The incoming wave angle was set per Smith (2007), and the directional spreading was accomplished using a Gaussian function. The spectral energy was the same along the open boundary. The model did not account for energy dissipation due to friction.

Model calibration and wave simulation

Due to the lack of data to calibrate the model, sufficient sensitivity on the wind velocity and direction was performed in order to obtain mean conditions on the resulting wave results. Several simulations we conducted for the duration of the storm; each wave simulation provided the distribution of significant wave heights, periods, and breaker indices. For each simulation, waves were propagated across the domain, and breaking wave conditions in the vicinity of the terminal lobe were recorded.

Sand transport

Breaking wave energy from all simulations was recorded in the domain by the model, as well as using the breaking criteria defined by Sverdrup and Munk (1946). Breaker angles were obtained by the model (wave direction prior to breaking), in relation to the orientation of the terminal lobe isobaths, breaker angles (15º – 45º) were computed for different breaker heights (0.5 – 2.75 m). Utilizing the relationship by Komar (1998), longshore current velocity at the mid-surf position (V_L) was calculated by

$$V_L = \sqrt{gH_{br}}\,\sin(a_b)\cos(a_b), \qquad (2)$$

where g is equal to acceleration due to gravity, H_{br} is the breaker height, and a_b is the breaker angle. The volumetric transport rate for quartz sand (Q_L) was then estimated by

$$Q_l = 0.088\rho g H_{br}{}^2 (V_L), \qquad (3)$$

where ρ is the density of seawater assumed to be approximately equal to 1,025 Kg/m^3, g is the acceleration due to gravity, and H_{br} is the breaker height. Calculated sand transport potential as a function of storm development during Hurricane Rita is shown in Supplementary Table DR1.

Supplementary Table DR1. Potential sand transport history as a function of storm development for hurricane Rita.

Time (hrs)	H_b (m)	α_b (^{o})	V_L (m/s)	Q_L (m^3/hr)	$Q_{L(cum)}$ (m^3/hr)
0	0.5	45	1.83	405	
6	1.5	35	2.57	5,125	16,592
12	2.2	25	2.30	9,838	44,889
18	2.8	22	2.28	15,234	75,214
24	2.2	15	1.41	6,025	63,776
30	1.5	15	1.16	2,313	25,013
40	0.5	35	1.49	329	13,207
				Total Transport	238,691

Supplementary References

Bretschneider, C.L., 1959, Hurricane design – wave practices: Transactions of the American Society of Civil Engineers, v. 124, p. 39–62.

Davis, J. C., 1986, Statistics and data analysis in geology, 2nd ed.: New York, John Wiley and Sons, 646 p.

Komar, P.D., 1998, Beach processes and sedimentation, 2nd ed.: New York, Prentice Hall, 544 p.

Krajewski, S. A. and Gibbs, B. L., 2003, Understanding Computer Contouring: Boulder, Gibbs and Associates, poster, 1 sheet.

Oceanweather Inc., 2006, Hindcast data on winds, waves, and currents in the northern Gulf of Mexico for hurricanes Katrina and Rita: Report submitted to the U.S. Department of Interior, Minerals Management Service, Herndon, VA, 174 p.

Smith, J.M., Sherlock, A.R., and Resio, D.T., 2001, STWAVE: Steady-state spectral wave model user's manual for STWAVE, Version 3.0: U.S. Army Corps of Engineers, Engineer Research and Development Center Report ERDC/CHL SR-01-1, 66 p.

Smith, J.M., 2007, Modeling nearshore waves for Hurricane Katrina: U.S. Army Engineer Research and Development Center, Technical Note ERDC/CHL-CHETN-I-76, 15 p.

Sverdrup, H.U. and Munk, W.H., 1946, Theoretical and empirical relations in forecasting breakers and surf: Transactions of the American Geophysical Union, v. 27, p. 828-836.